Matter and Radiation at Extremes | RESEARCH ARTICLE | scitation.org/journal/mre

First-principles study on the electronic structure transition of β-UH_3 under high pressure

Cite as: Matter Radiat. Extremes 7, 058402 (2022); doi: 10.1063/5.0091969
Submitted: 19 March 2022 • Accepted: 21 June 2022 •
Published Online: 1 August 2022

Juefei Wu, Wang Yue-Chao, Yu Liu, Bo Sun, Yanhong Zhao, Jiawei Xian, Xingyu Gao,[a] Haifeng Liu, and Haifeng Song[a]

AFFILIATIONS

Laboratory of Computational Physics, Institute of Applied Physics and Computational Mathematics, Beijing 100088, China

Note: This paper is a part of the Special Topic Collection on High Pressure Science 2022.
[a]**Authors to whom correspondence should be addressed:** gao_xingyu@iapcm.ac.cn and song_haifeng@iapcm.ac.cn

ABSTRACT

We investigate the electronic properties of stable β-UH_3 under high pressure up to 75 GPa within the first-principles DFT + U formalism with pressure-dependent U in a self-consistent calculation, and we find an electronic structure transition at about 20 GPa due to the quantum process of localization and itinerancy for partially filled uranium 5f electrons. The electronic structure transition is examined from four perspectives: magnetization, band structure, density of states, and 5f electron energy. On the basis of the density of states of 5f electrons, we propose an order parameter, namely, the 5f electron energy, to quantify the electronic structure transition under pressure. Analogously to the isostructural transition in 3d systems, β-UH_3 retains its magnetic order after the electronic structure transition; however, this is not accompanied by volume collapse at the transition point. Our calculation is helpful for understanding the electronic properties of β-UH_3 under high pressure.

I. INTRODUCTION

Hydrogen-rich materials synthesized under high pressure such as H_3S,[1] LaH_{10},[2] and the C–S–H system[3] have opened possible routes to high-temperature superconductivity. The uranium–hydrogen binary system is among the potential candidates for such materials.[4] Kruglov *et al.*[4] synthesizied the predicted UH_7 and UH_8 in laser-heating diamond anvil cell (DAC) experiments, using UH_3 as the precursor material. UH_3 is a stable composition under ambient conditions[5–8] and has important roles in nuclear technology and as a chemical hydrogen storage material.[9–13] Therefore, exploring the high-pressure properties of UH_3 is important for both fundamental research and industrial applications.[5]

At present, there is a fairly comprehensive understanding of UH_3 under ambient condition. UH_3 crystallizes in two structures: α-UH_3 and β-UH_3.[14] The α-UH_3 structure is metastable and can only be found at low temperatures.[15] It transforms into stable β-UH_3 at temperatures between 373 and 523 K.[16] Taylor *et al.*[15] simulated the phase transformation paths from α-UH_3 to β-UH_3. Tkach *et al.*[17] stabilized α-UH_3 with Zr and conducted experiments to study its electronic properties. β-UH_3 transforms from a ferromagnetic (FM) state[18] to a paramagnetic (PM) state at a Curie temperature of about 180 K.[19] Zhang *et al.*[16] calculated the electronic, mechanical, and thermodynamic properties of both UH_3 phases under ambient conditions.

Zhang *et al.*[20] calculated the mechanical and thermodynamic properties of α-UH_3 under high pressures. According to DAC experiments,[4,21] α-UH_3 transforms to β-UH_3 when the pressure is increased to 5 GPa, and the x-ray diffraction signature of β-UH_3 is preserved up 69 GPa.[4] According to theoretical calculations by Taylor,[22] ferromagnetism in β-UH_3 vanishes when the unit-cell volume becomes about 50% of the equilibrium volume. In particular, the magnetization exhibits a sharp decrease from about 2.8 to 2.0 μ_B/U as the volume of the system increases from 32 to 36 $Å^3$.[22] These characteristics of the magnetization appear to be analogous to the isostructural transitions in 3d materials such as $FeCO_3$[23] and $LiFePO_4$.[24] In Refs. 23 and 24, the structure was retained, while the spin state was transformed from a high-spin (HS, $S = 2$) to a low-spin (LS, $S = 0$) state under pressure, accompanied by volume collapse at the transition point. Actually, the magnetic order of β-UH_3 remains ferromagnetic, and the impact of the transition

on the volume is not known at present. Besides, β-UH_3 contains 5f electrons,[25,26] and this gives rise to exotic physics.[27] Thus, it is intriguing to study the electronic structures of β-UH_3 under high pressure.

In this work, we conduct first-principles calculations of the electronic structure of β-UH_3 under high pressure. A local screened Coulomb correction (LSCC) approach[28] is employed to evaluate the pressure-dependent local Coulomb interaction parameters in a self-consistent way. We predict an electronic structure transition of β-UH_3 under high pressure and illustrate it from four perspectives. First, we find that the magnetization has a discontinuity around 32 Å^3, suggesting a possible electronic structure transition. Second, we find that the calculated band structure of β-UH_3 is reconstructed after 18 GPa. Third, after the transition, the density of states (DOS) becomes more dispersed. Fourth, we present an order parameter to quantify the electronic structure transition by calculating the 5f electron energy of the occupied states under pressure. Finally, we analyze the charge density difference to reveal the enhanced metallicity and calculate the volume drop after the transition.

II. COMPUTATIONAL METHODS

The space group of the stable β-UH_3 structure is $Pm\bar{3}n$ (223),[29,30] with the uranium atoms occupying the 2(a) (0, 0, 0) [U(I)] and 6(c) (0.25, 0, 0.5) [U(II)] sites, and the hydrogen atoms occupying the 24(k) (0, 0.156, 0.313) sites.[21,31]

In the present *ab initio* calculations, we employ the Vienna *Ab initio* Simulation Package (VASP) based on density functional theory (DFT).[32,33] The exchange-correlation functional is treated using the generalized gradient approximation (GGA) of Perdew, Burke, and Ernzerhof.[34] The calculations use the projector-augmented wave (PAW)[35] approach to describe the core electrons and their effects on valence orbitals. Spin–orbit coupling (SOC) is taken into account, with the direction of magnetic axis along (111). Ferromagnetic (FM) ordering is assumed in the simulation [Fig. 1(a)].

DFT + U[36] calculations are performed using the formulation of Dudarev *et al.*[37] to account for the on-site Coulomb repulsion among the localized uranium 5f electrons. The total energy is of the form

$$E_{\mathrm{LSDA}+U} = E_{\mathrm{LSDA}} + \frac{U-J}{2}\sum_{\sigma}\left[\mathrm{Tr}\,\rho^{\sigma} - \mathrm{Tr}\left(\rho^{\sigma}\rho^{\sigma}\right)\right], \tag{1}$$

where ρ^{σ} is the local density matrix of the f states, and the Hubbard U and Hund exchange J correspond to the spherically averaged screened Coulomb interaction and the exchange interaction, respectively. The difference between U and J is significant in this formalism and is denoted by U_{eff} for simplicity. The dependence of U on pressure or volume is evaluated by the LSCC approach,[28] which provides accurate descriptions of electronic and magnetic properties in strongly correlated systems.

To estimate the Curie temperature T_{C}, we use the classical Heisenberg model in mean-field theory (MFA).[38] The Curie temperature is given by

$$T_{\mathrm{C}} = \frac{2zJS(S+1)}{3k_{\mathrm{B}}} = \frac{E_{\mathrm{AFM}} - E_{\mathrm{FM}}}{6k_{\mathrm{B}}}, \tag{2}$$

where k_{B} is the Boltzmann constant, and E_{FM} and E_{AFM} are the total energies (per formula unit) of the FM and antiferromagnetic (AFM) states [Fig. 1(b)], respectively. To verify the feasibility of the AFM state, we construct a magnetic disorder 2 × 2 × 2 supercell using the similar atomic environment (SAE) method.[39] Five components [H][U(-1-11)][U(11-1)][U(-111)][U(1-1-1)] are considered and are randomly distributed in the supercell.

We recheck our electronic structure calculations using the orbital polarization (OP) limit of GGA + U.[16]

We set the plane-wave kinetic-energy cutoff to 650 eV, and the Brillouin zone is sampled with a special k-mesh generated by the Monkhorst–Pack scheme with a k-point spacing of $2\pi \times 0.03$ Å^{-1}. The convergence tolerance is 10^{-6} eV for total energy, and all forces are converged to be less than 0.003 eV/Å.

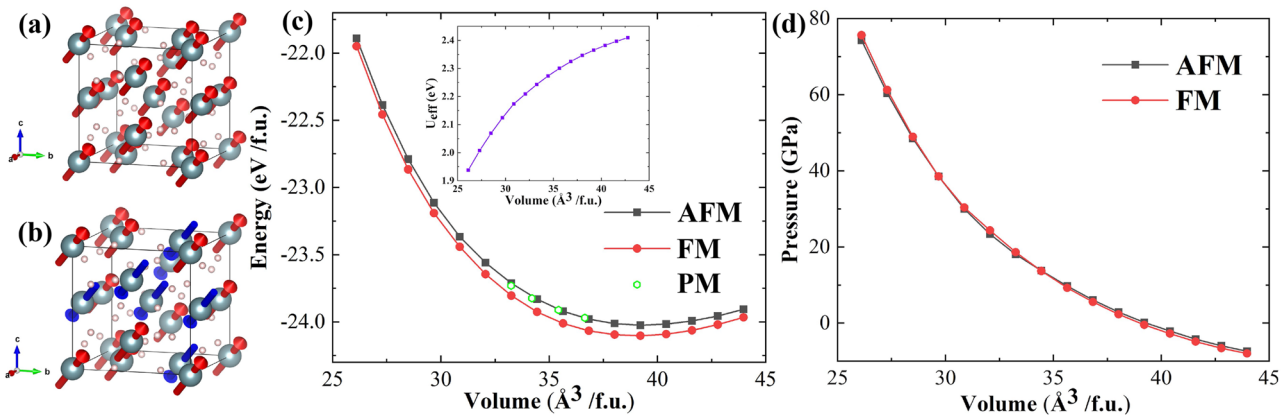

FIG. 1. (a) and (b) Magnetic structures of the FM and AFM states, respectively, with the red and blue arrows denoting the magnetic axes. (c) Energy–volume relations of the FM, AFM, and PM states. The inset shows U_{eff} as determined by the LSCC approach under different pressures. (d) Pressure–volume relations of FM and AFM states.

III. RESULTS AND DISCUSSION

High-pressure experimental[4,21] and theoretical[5] studies suggest that there is no structural transition in β-UH_3 up to 69 GPa. In our calculation, the structure remains $Pm\bar{3}n$ in the structural relaxation process. The calculated spontaneous magnetization under ambient conditions is 0.68 μ_B/U. This is close to the experimental value of ~1 μ_B/U[17] and is in line with the results calculated using the OP limit method.[16] As plotted in Fig. 1, the total energy of the FM state is below that of the AFM state, and U_{eff} gradually decreases from about 2.4 to 1.9 eV with increasing pressure (inset of Fig. 1). The E–V relation indicates that the ground state retains FM order in the calculated pressure range. The supercell constructed by the SAE method is able to describe the PM state, and the total energy difference between the PM and AFM states is less than 0.1%. This indicates that the AFM order is a good approximation to the PM state.[40] To estimate the Curie temperature T_C, we calculate the total energies of the FM and AFM states with a fixed U_{eff} = 2.3 estimated at ambient pressure. The calculated Curie temperature is 158.8 K, which is in reasonable agreement with the experimental value of 180 K.[16] Thus, our method is suitable for simulating the properties of β-UH_3.

We present the electron magnetization per uranium atom in Fig. 2. The discontinuity in magnetization is around 20 GPa, and the magnitude is about 0.14 μ_B/U. The pressure of 20 GPa corresponds to about 33 Å^3. The reduction in magnetization indicates a possible electronic structure transition, and the abrupt change around 33 Å^3 suggests an immediate elevation of metallicity.

To illustrate the transition, we calculate the band structures of β-UH_3 at pressures up to 75 GPa, as plotted in Fig. 3. The band structures below 18 GPa have analogous characteristics, such as a "bandgap" along the Brillouin path X–R. We can also observe a gradual variation in the band structure from 24 to 75 GPa.

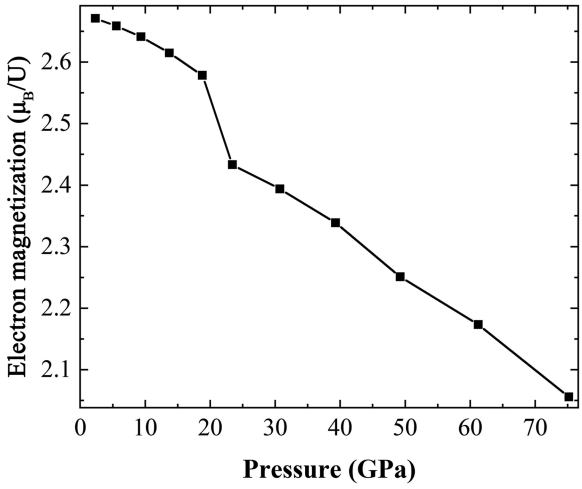

FIG. 2. Electron magnetization per uranium atom as a function of pressure for β-UH_3.

Here, we characterize two types of electronic structure. One, E1, exhibits a "bandgap" along X–R, as exemplified by the band structures at pressures below 18 GPa [Figs. 3(a)–3(c)]. The other, E2, lacks this "bandgap," as exemplified by the band structures at pressures above 24 GPa [Figs. 3(d)–3(f)]. From a comparison of E1 at 18 GPa [Fig. 3(c)] with E2 at 24 GPa [Fig. 3(d)], it can be seen that the "bandgap" along X–R undergoes a sudden collapse. The band structure is reconstructed along other Brillouin paths as well. This

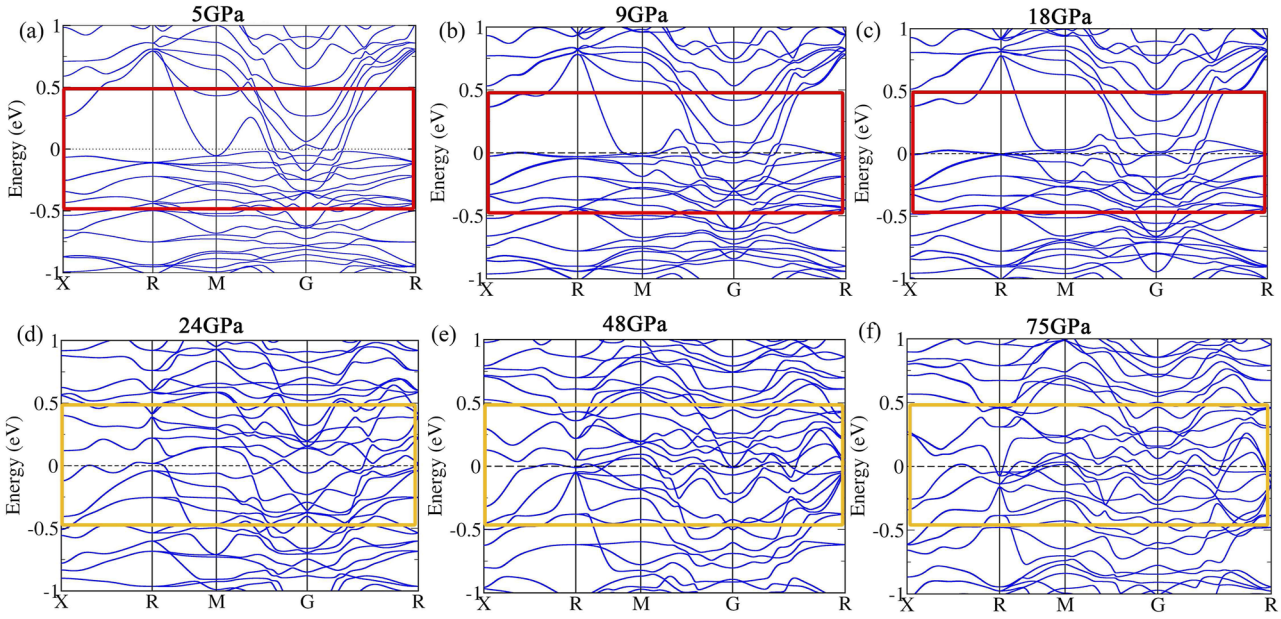

FIG. 3. Band structures of β-UH_3 under different pressures.

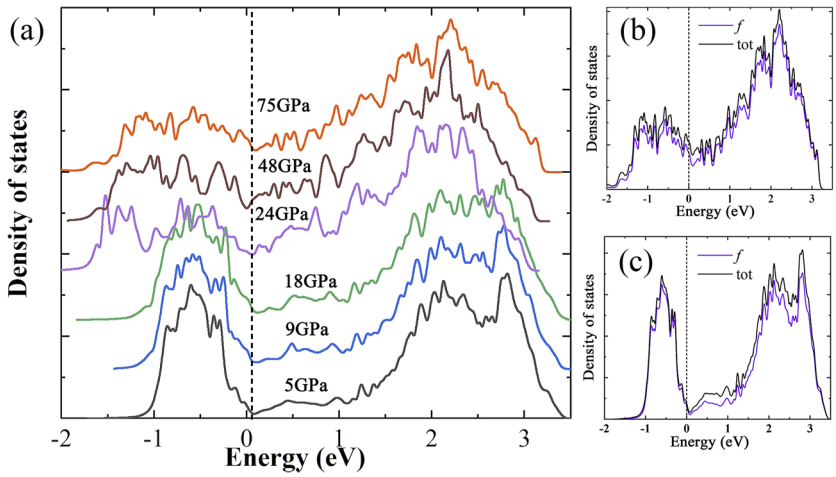

FIG. 4. (a) DOS of β-UH_3 under different pressures relative to the Fermi energy. (b) and (c) Total f-electron DOS at 75 and 5 GPa, respectively.

suggests the existence of a transition in electronic structure between 18 and 24 GPa.

We then calculate the DOS of β-UH_3 under different pressures [Fig. 4(a)]. At each pressure, the DOS is relative to the Fermi energy. As can be seen from Fig. 4(a), the distribution below 18 GPa is relatively localized, while that above 24 GPa becomes more dispersed. In Figs. 4(b) and 4(c), the f electrons make the greatest contribution in both the E1 and E2 states around the Fermi energy. Hence, the dispersed behavior above 24 GPa, such as the emerging peaks around −1.5 eV at 24 GPa [Fig. 4(a)], can be attributed to the redistribution of 5f electrons.

To quantify the electronic structure transition, we propose the following order parameter:

$$E_{5f} = \frac{\int_{-\infty}^{E_F} E N_f(E) dE}{\int_{-\infty}^{E_F} N_f(E) dE} - E_F, \tag{3}$$

where $N_f(E)$ is the DOS of 5f electrons and E_F is the Fermi energy. This order parameter is also referred to as the 5f electron energy. As depicted in Fig. 5, there is a cliff in the 5f electron energy around 20 GPa. The height of this cliff is about 0.36 eV, which is comparable to the value of the energy at 18 GPa (−1.03 eV) and 24 GPa (−1.39 eV). This sharp drop is related to the sudden broadening of the 5f bands, indicating enhancement of the itinerancy. The order parameter based on the 5f electron energy can be an appropriate descriptor for the electronic structure transition.

We calculate the enthalpy of the distinct electronic states and determine the transition point at 21 GPa. At this pressure, we analyze the charge density difference between E1 and E2 states. As illustrated in Fig. 6, we select the (200) plane, the isosurface value is ±0.001 e/bohr,[3] and blue and red colors represent areas losing and gaining electrons, respectively. The areas losing electrons are localized around uranium and hydrogen atoms, while the areas gaining most electrons are connected via the H–U(II)–U(II)–H channel. Hence, the E2 state is more itinerant than the E1 state; in

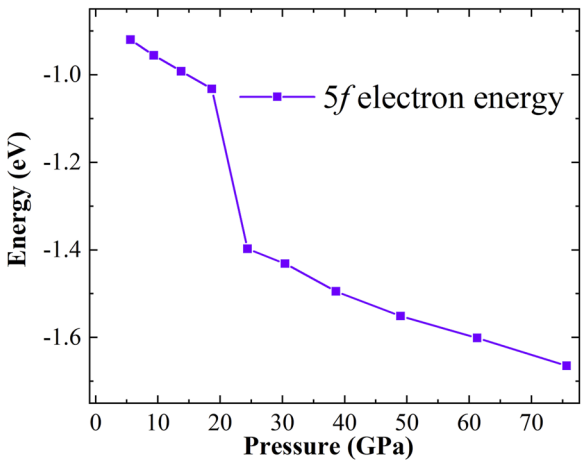

FIG. 5. 5f electron energy of occupied states under different pressures.

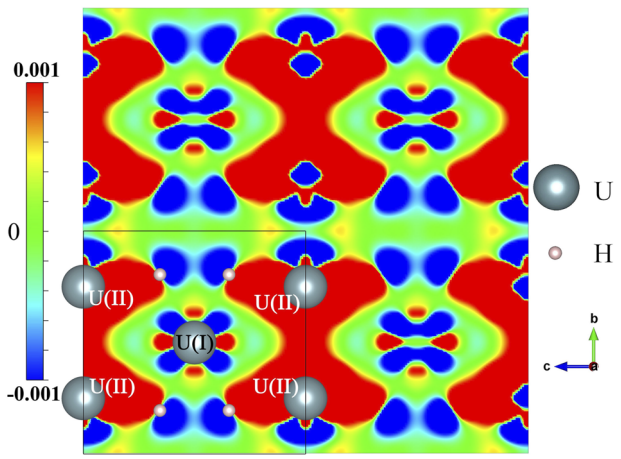

FIG. 6. Charge density difference of β-UH_3 relative to E1 state on the (200) plane at 21 GPa.

other words, the metallicity is elevated after the electronic structure transition.

We recheck the electronic structure calculations with the OP limit of GGA + U.[16] The ground state retains FM order within 70 GPa, and we can observe an electronic structure transition around 13 GPa (33 Å^3) as well. This confirms the validity of the electronic structure transition under high pressure for β-UH_3. Besides, the volume drops about 0.7% at the transition point, which is significantly less than the 10% drop for $FeCO_3$[23] and the 3% drop for $LiFePO_4$.[24] This may explain why volume collapse has not reported in previous high-pressure experiments.[4,21]

To further verify the electronic structure transition in β-UH_3, we suggest that detailed partial fluorescence yield x-ray absorption spectroscopy (PFY XAS) or resonant inelastic x-ray scattering (RIXS) spectra under pressure be performed in the future.

IV. CONCLUSIONS

In summary, using first-principles calculations, we have predicted an electronic structure transition in β-UH_3 at about 20 GPa, and we have illustrated this from the perspectives of magnetization, band structure, DOS, and 5f electron energy. On the basis of the 5f electron energy, we propose an order parameter as a descriptor for the electronic structure transition. After the electronic structure transition, the itinerancy of the 5f electrons exhibits a sudden enhancement, accompanied by an abrupt elevation in metallicity. β-UH_3 remains ferromagnetic after the electronic structure transition, and this transition has only a slight impact on the structure volume. Our calculations provide further understanding of the electronic properties of β-UH_3 under high pressure.

ACKNOWLEDGMENTS

We acknowledge support from the National Key Research and Development Program of China under Grant No. 2021YFB3501503 and from the National Natural Science Foundation of China under Grant Nos. 12004048 and U1930401.

AUTHOR DECLARATIONS

Conflict of Interest

The authors have no conflicts to disclose.

Author Contributions

Juefei Wu: Investigation (equal); Writing – original draft (equal); Writing – review & editing (equal). **Wang Yue-Chao:** Investigation (equal); Writing – original draft (equal); Writing – review & editing (equal). **Yu Liu:** Writing – original draft (supporting). **Bo Sun:** Writing – original draft (equal); Writing – review & editing (equal). **Yanhong Zhao:** Writing – original draft (equal); Writing – review & editing (equal). **Jiawei Xian:** Writing – original draft (equal); Writing – review & editing (equal). **Xingyu Gao:** Project administration (equal); Writing – original draft (equal); Writing – review & editing (equal). **Haifeng Liu:** Writing – original draft (equal); Writing – review & editing (equal). **Haifeng Song:** Supervision (lead); Writing – review & editing (supporting).

DATA AVAILABILITY

The data that support the findings of this study are available from the corresponding authors and Wu upon reasonable request.

REFERENCES

[1] A. P. Drozdov, M. I. Eremets, I. A. Troyan, V. Ksenofontov, and S. I. Shylin, "Conventional superconductivity at 203 kelvin at high pressures in the sulfur hydride system," Nature **525**, 73–76 (2015).
[2] M. Somayazulu, M. Ahart, A. K. Mishra, Z. M. Geballe, M. Baldini, Y. Meng, V. V. Struzhkin, and R. J. Hemley, "Evidence for superconductivity above 260 K in lanthanum superhydride at megabar pressures," Phys. Rev. Lett. **122**, 027001 (2019).
[3] E. Snider, N. Dasenbrock-Gammon, R. McBride, M. Debessai, H. Vindana, K. Vencatasamy, K. V. Lawler, A. Salamat, and R. P. Dias, "Room-temperature superconductivity in a carbonaceous sulfur hydride," Nature **586**, 373–377 (2020).
[4] I. A. Kruglov, A. G. Kvashnin, A. F. Goncharov, A. R. Oganov, S. S. Lobanov, N. Holtgrewe, S. Jiang, V. B. Prakapenka, E. Greenberg, and A. V. Yanilkin, "Uranium polyhydrides at moderate pressures: Prediction, synthesis, and expected superconductivity," Sci. Adv. **4**, eaat9776 (2018).
[5] X. Wang, M. Li, F. Zheng, and P. Zhang, "Crystal structure prediction of uranium hydrides at high pressure: A new hydrogen-rich phase," Phys. Lett. A **382**, 2959–2964 (2018).
[6] M. Liu, Y. Shi, M. Liu, D. Li, W. Mo, T. Fa, B. Bai, X. Wang, and X. Chen, "First-principles comprehensive study of electronic and mechanical properties of novel uranium hydrides at different pressures," Prog. Nat. Sci.: Mater. Int. **30**, 251–259 (2020).
[7] P. F. Souter, G. P. Kushto, L. Andrews, and M. Neurock, "Experimental and theoretical evidence for the formation of several uranium hydride molecules," J. Am. Chem. Soc. **119**, 1682–1687 (1997).
[8] J. Raab, R. H. Lindh, X. Wang, L. Andrews, and L. Gagliardi, "A combined experimental and theoretical study of uranium polyhydrides with new evidence for the large complex $UH_4(H_2)_6$," J. Phys. Chem. **111**, 6383–6387 (2007).
[9] D. Chung, J. Lee, D. Koo, H. Chung, K. H. Kim, H.-G. Kang, M. H. Chang, P. Camp, K. J. Jung, S. Cho, S.-H. Yun, C. S. Kim, H. Yoshida, S. Paek, and H. Lee, "Hydriding and dehydriding characteristics of small-scale DU and ZrCo beds," Fusion Eng. Des. **88**, 2276–2279 (2013).
[10] A. Banos, N. J. Harker, and T. B. Scott, "A review of uranium corrosion by hydrogen and the formation of uranium hydride," Corros. Sci. **136**, 129–147 (2018).
[11] H. Yoo, W. Kim, and H. Ju, "A numerical comparison of hydrogen absorption behaviors of uranium and zirconium cobalt-based metal hydride beds," Solid State Ionics **262**, 241–247 (2014).
[12] F. D. Manchester and A. San-Martin, "The H-U (hydrogen-uranium) system," J. Phase Equilib. **16**, 263–275 (1995).
[13] J. Bloch, "The hydriding kinetics of activated uranium powder under low (near equilibrium) hydrogen pressure," J. Alloys Compd. **361**, 130–137 (2003).
[14] R. N. R. Mulford, F. H. Ellinger, and W. H. Zachariasen, "A new form of uranium hydride," J. Am. Chem. Soc. **76**, 297 (1954).
[15] C. D. Taylor, T. Lookman, and R. S. Lillard, "Ab initio calculations of the uranium–hydrogen system: Thermodynamics, hydrogen saturation of α-U and phase-transformation to UH_3," Acta Mater. **58**, 1045–1055 (2010).
[16] Y. Zhang, B. Wang, Y. Lu, Y. Yang, and P. Zhang, "Electronic, mechanical and thermodynamic properties of α-UH_3: A comparative study by using the LDA and LDA+U approaches," J. Nucl. Mater. **430**, 137–141 (2012).
[17] I. Tkach, M. Paukov, D. Drozdenko, M. Cieslar, B. Vondráčková, Z. Matěj, D. Kriegner, A. V. Andreev, N.-T. H. Kim-Ngan, I. Turek, M. Diviš, and L. Havela, "Electronic properties of α-UH_3 stabilized by Zr," Phys. Rev. B **91**, 115116 (2015).
[18] R. Troc and W. Suski, "The discovery of the ferromagnetism in U(H, D)$_3$: 40 years later," J. Alloys Compd. **219**, 1 (1995).
[19] J. Prchal, V. Buturlim, J. Valenta, M. Dopita, M. Divis, I. Turek, L. Kyvala, D. Legut, and L. Havela, "Pressure variations of the 5f magnetism in UH_3," J. Magn. Magn. Mater. **497**, 165993 (2019).

[20]C. Zhang, H. Jiang, H.-L. Shi, G.-H. Zhong, and Y.-H. Su, "Mechanical and thermodynamic properties of α-UH_3 under pressure," J. Alloys Compd. **604**, 171–174 (2014).
[21]I. Halevy, S. Salhov, S. Zalkind, M. Brill, and I. Yaar, "High pressure study of β-UH_3 crystallographic and electronic structure," J. Alloys Compd. **370**, 59–64 (2004).
[22]C. D. Taylor, "Characterizing electronic structure motifs in β-UH_3," Phys. Rev. B **82**, 224408 (2010).
[23]H. Shi, W. Luo, B. Johansson, and R. Ahuja, "First-principles calculations of the electronic structure and pressure-induced magnetic transition in siderite $FeCO_3$," Phys. Rev. B **78**, 155119 (2008).
[24]M. Núñez Valdez, I. Efthimiopoulos, M. Taran, J. Müller, E. Bykova, C. McCammon, M. Koch-Müller, and M. Wilke, "Evidence for a pressure-induced spin transition in olivine-type $LiFePO_4$ triphylite," Phys. Rev. B **97**, 184405 (2018).
[25]T. Gouder, R. Eloirdi, F. Wastin, E. Colineau, J. Rebizant, D. Kolberg, and F. Huber, "Electronic structure of UH_3 thin films prepared by sputter deposition," Phys. Rev. B **70**, 235108 (2004).
[26]G. Zwicknagl, "5*f* electron correlations and core level photoelectron spectra of uranium compounds," Phys. Status Solidi B **250**, 634–637 (2013).
[27]L. Huang and H. Lu, "Pressure-driven 5*f* localized-itinerant transition and valence fluctuation in cubic phase californium," Phys. Rev. B **99**, 045109 (2019).
[28]Y.-C. Wang and H. Jiang, "Local screened Coulomb correction approach to strongly correlated *d*-electron systems," J. Chem. Phys. **150**, 154116 (2019).
[29]R. E. Rundle, "The structure of uranium hydride and deuteride," J. Am. Chem. Soc. **69**, 1719–1723 (1947).
[30]R. E. Rundle, "The hydrogen positions in uranium hydride by neutron diffraction," J. Am. Chem. Soc. **73**, 4172–4174 (1951).
[31]J. Grunzweig-Genossar, M. Kuznietz, and B. Meerovici, "Nuclear magnetic resonance in uranium hydride and deuteride," Phys. Rev. B **1**, 1958 (1970).
[32]G. Kresse and J. Furthmüller, "Efficient iterative schemes for *ab initio* total-energy calculations using a plane-wave basis set," Phys. Rev. B **54**, 11169 (1996).
[33]H. J. Monkhorst and J. D. Pack, "Special points for Brillouin zone integrations," Phys. Rev. B **13**, 5188 (1976).
[34]J. P. Perdew, K. Burke, and M. Ernzerhof, "Generalized gradient approximation made simple," Phys. Rev. Lett. **77**, 3865 (1996).
[35]P. E. Blöchl, "Projector augmented-wave method," Phys. Rev. B **50**, 17953 (1994).
[36]V. I. Anisimov, J. Zaanen, and O. K. Andersen, "Band theory and Mott insulators: Hubbard U instead of Stoner I," Phys. Rev. B **44**, 943 (1991).
[37]S. L. Dudarev, G. A. Botton, S. Y. Savrasov, C. J. Humphreys, and A. P. Sutton, "Electron-energy-loss spectra and the structural stability of nickel oxide: An LSDA+U study," Phys. Rev. B **57**, 1505 (1998).
[38]A. H. Morrish, *The Physical Principles of Magnetism* (John Wiley & Sons, New York, London, Sydney, 1965).
[39]F. Tian, D.-Y. Lin, X. Gao, Y.-F. Zhao, and H.-F. Song, "A structural modeling approach to solid solutions based on the similar atomic environment," J. Chem. Phys. **153**, 034101 (2020).
[40]B. Dorado and P. Garcia, "First-principles DFT+U modeling of actinide-based alloys: Application to paramagnetic phases of UO_2 and (U, Pu) mixed oxides," Phys. Rev. B **87**, 195139 (2013).